Progress In Electromagnetics Research C, Vol. 127, 1–16, 2022

TV-Based Phased Array System Design in BTSs for 5G/IoT Applications

Amir R. Dastkhosh[1, *], Mehdi Naseh[2], Davide Dardari[2], and Fujiang Lin[1]

Abstract—Cellular UHF (Ultra High Frequency) transceiver networks and base transceiver station antenna systems comprise high power phase shifters for changing and adjusting the phases or delays of high-power transmitting signals delivered to antenna elements. In this work, theoretical and practical adjustment methods of amplitudes and phases for electronic steering of a high power phased array antenna pattern are illustrated. In addition, a high power phase shifter with an asymmetric power divider is designed. The phases are changed and adjusted progressively, and thus the beam direction changes from $-60°$ to $60°$. The UHF phase shifter has been simulated with Advanced Design System (ADS) and CST STUDIO SUITE SPARK3D and measured. The simulations show that the designed and manufactured UHF phase shifter can also handle more than 20 kW and can be redesigned to reach up to more than 100 kW RF (Radio Frequency) power (microstrip/stripline structures) and can control/change phases of transmitting /receiving antennas. The phase shifter can be designed on any low loss substrate. By using this method in planar high power phased array antenna systems, $360°$ planar beam tilting is also achievable.

1. INTRODUCTION

In the following years, the demands for ultra-high data rate in mobile and wireless communications and tools will be booming. For reaching the hundreds of Exabyte, next mobile generations and new cellular communication systems will meet such requirements. Using new spectrum beyond sub-6 GHz frequencies could be one way to address this rising demand and satisfy the needs of greater than 10 Gbps peak and edge speeds of approaching 100 Mbps for extreme mobile broadband (eMBB) applications [1–5]. Furthermore, for optimal performance, wireless sensor networks such as ZigBee, LDWA, LoRa, WWAN, and mobile radio networks such as 2G, 3G, 4G, and soon 5G/6G (5th/6th Generation) require online data processing, artificial intelligence (AI), and machine learning (ML), and all of them need super ultra-wideband communication instruments and systems.

The advantages of conducting super ultra-wideband and high-performance networks are (Figs. 1–2 and Tables 1–2): Robotic, indoor wireless localization, autonomous vehicles (self-driving cars or with logistics management purposes), virtual reality (VR), that the time delay is a crucial factor, agricultural machinery and intelligent products traceability, smart homes and future Internet of Things (IoT) such as tags and UHF IoT radio frequency identification (I-RFID) by meandering angle antennas, energy harvesting among massive systems, creating several networks for multi-purpose use or network slicing, public safety, and so on.

Furthermore, in a complex real-time environment, IoT devices must be intelligently managed, and 5G wireless networks must provide ultra-reliable, low-latency communication. Where a content has

Received 19 September 2022, Accepted 4 November 2022, Scheduled 21 November 2022

* Corresponding author: Amir Reza Dastkhosh (amirreza@mail.ustc.edu.cn).

[1] Department of Electronic Science and Technology, Micro-/Nano Electronic System Integration R&D Centre (MESIC), University of Science and Technology of China, Hefei, China. [2] Department of Electrical, Electronic, and Information Engineering, "Guglielmo Marconi" — DEI, University of Bologna, Bologna, Italy.

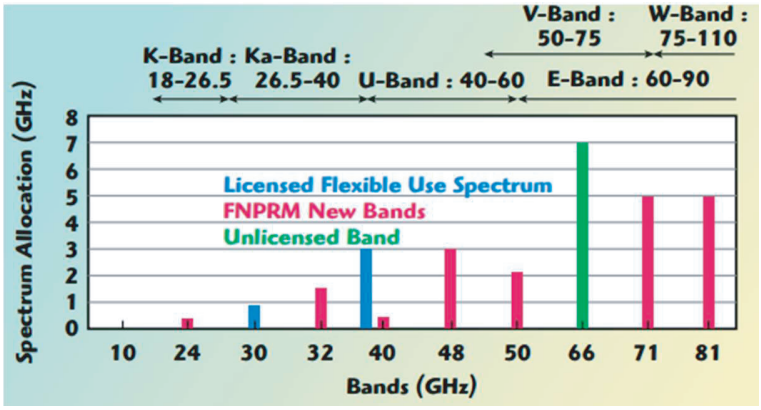

Figure 1. Proposed 5G mmWave spectrum.

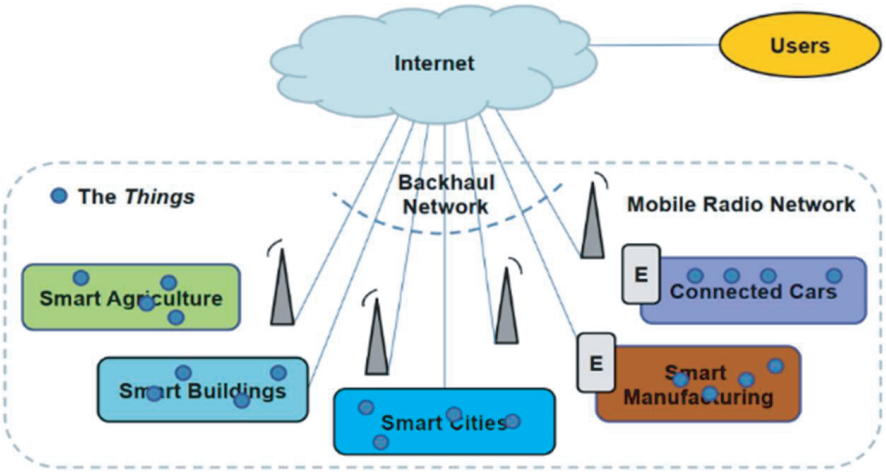

Figure 2. IoT and 5G.

Table 1. 5G frequencies.

Band	Frequency (MHz)	Type
FR1	450–6000	Sub-6 GHz
FR2	24250–52600	mm-Wave

to be distributed to a massive number of devices, instead of unicast, broadcast has to be utilized. In broadcast networks such as TV broadcasting, a massive number of users receive the transmitted signal from the communication towers, and the capacity of the transceivers does not depend on their clientele. Over-the-top (OTT) companies like Netflix and HBO are now entering the media market and producing on-demand content.

In addition, there are many devices including smartphones and tablets and possible ways that by using them, someone can watch TV. In 2012, the International Telecommunication Union (ITU) reallocated the 700 MHz band from digital terrestrial (DTT) to mobile internet, ranging from 694 to 790 MHz. A combination of IP- and non-IP TV-distribution platforms develops and distributes evenly in the 5G era. Capacity optimization for the Evolved Multimedia Broadcast Multicast Service (eMBMS) Broadcast is a critical necessity for the ever-increasing demand for mobile data. Theoretically, the (LTE) Supplemental Downlink (SDL) idea might be used to accelerate the implementation of the standard 700-MHz DD2 bands for MBB by allowing for improved cohabitation with TV transmitters (Tables 3–5).

Table 2. Typical wireless systems and their specifications.

Wireless System	Specifications
Long Range Systems: Sigfox	• Since few years. • Proprietary solution. • (Much) Below-MHz user throughput. • Energy consumption has been optimized. • Network Operator (Sigfox). • 868 MHz ISM band.
Long Range Systems: LoRa	• Since few years. • Proprietary solution/LoRa Alliance. • (Much) Below-MHz user throughput. • Energy consumption has been optimized. • Network Operator not needed. • 868 MHz ISM band.

Table 3. A typical DVB-T and 5G channeling (700/800 MHz in Europe/Americas).

DVB-TV			5G		
470–478	...	686–694	694–708	...	862–869

Table 4. A typical reframed 700 MHz scheme.

DVB-T/T2 for Terrestrial TV	470 MHz–608 MHz	614 MHz–694 MHz
eMBMS for Terrestrial TV (Higher Efficiency)	470 MHz–608 MHz	
New Spectrum Feed-up Use/5G (Higher Efficiency)		614 MHz–694 MHz

Table 5. Typical Digital Terristrial Broadcasting (DTTB) system parameters.

Parameters	Value
EIRP (Equivalent Isotropically Radiated Power) DTT	• High Power Transmitter: 200 kW • Medium Power Transmitter: 5 kW
DTT Height	• High Power Transmitter: 200 m • Medium Power Transmitter: 75 m

Providing TV-based foundations in UHF/VHF (very high/ultra-high) frequencies that reuse the TV white space (TVWS) channels and have substantially reduced free space loss is one approach (at least 10 dB because the frequency is 10 times lower). This matter leads to digital TV broadcasting over cellular networks or LTE enTV (enhanced TV) and implementing 5G simultaneously. Actually, release 14/(16) LTE enTV meets most of the 5G new radio (NR) and EU digital TV broadcast requirements and is especially interesting for Europe, because of reusing the 700 MHz frequency band (typically using 600–800 MHz). As mentioned, it also causes leveraging existing networks and resources optimally for cellular networks, TV broadcasters, and content providers to access richer content on their mobile or

fixed devices. The outcome of the 600-MHz TV for mobile broadband auction, particularly in the United States, determines if a comparable process for satellite to mobile broadband is plausible and cost-effective.

On the other hand, the Internet of Things (IoT) as an application is a self-configuring, adaptable, complex dynamic network that uses common communication protocols to link things to the Internet. The IoT is becoming omnipresent, covering all sectors of people's lives. These connectivity criteria, as well as mobile edge and core intelligence, can be realized by combining basic principles of Artificial Intelligence (AI) and Machine Learning (ML) through wireless networks and end-user devices. Also, full-dimension multiple-input multiple-output (FD-MIMO) technology is one of the key enabling technologies for the future 5G. Fig. 3 depicts some common wireless systems as well as their specifications. Figs. 4–5 illustrate the transceiver structure of a 5G wireless network [5–10]. The evolution of cellular systems such as 5G new radio and Long Term Evolution systems lead to thriving innovative cellular systems and versatile patents in communications (like MIMO, spatial multiplexing). In cellular systems, performance is determined by certain variables and methods such as antenna gain, diversity gain, interference

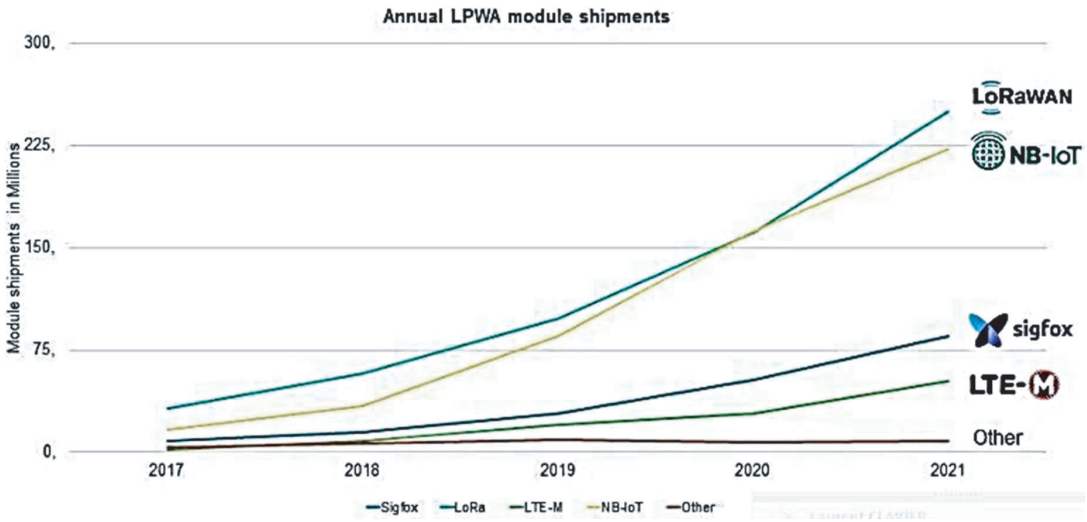

Figure 3. IoT and wireless sensors.

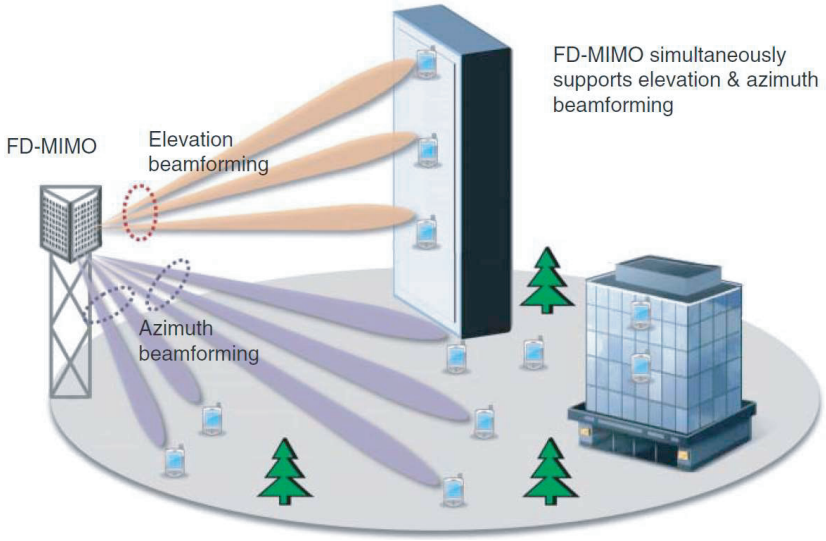

Figure 4. A MIMO system.

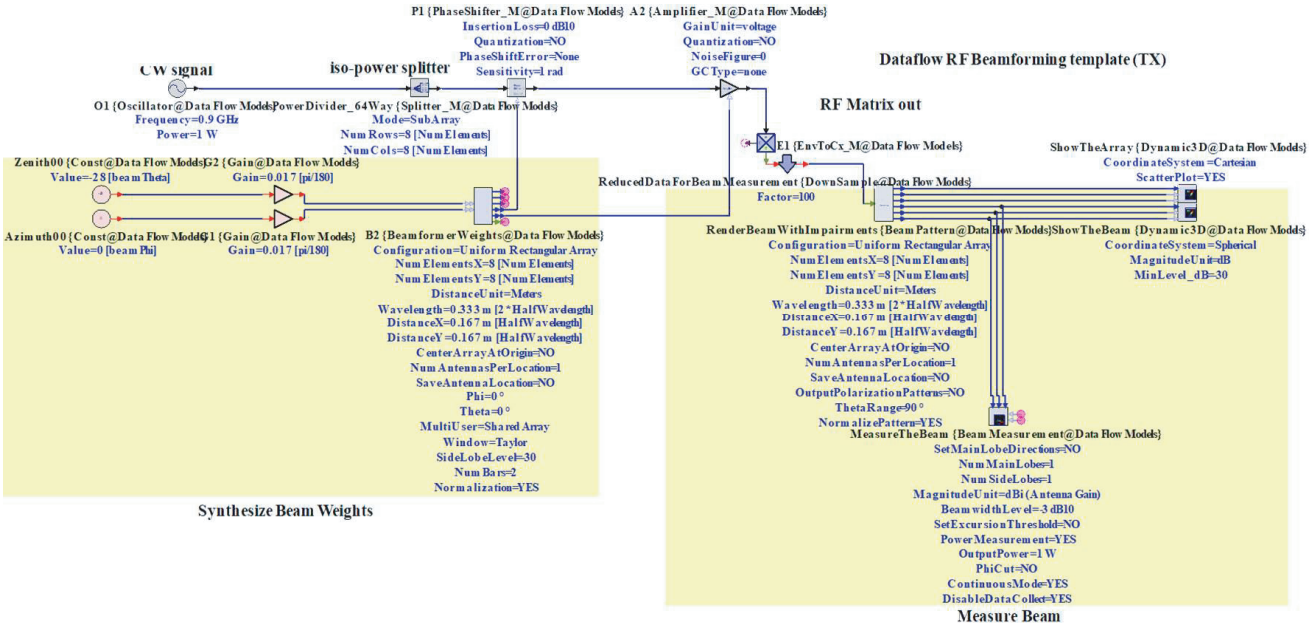

Figure 5. Beamformer/direction finder parts.

suppression (increasing the signal-to-interference-plus-noise ratio (SINR) and improve link reliability and robustness), beamforming (focusing antenna beam straight to the user), multiplexing gain (multi-stream transmission) or space division multiple access (SDMA), beam tracking (that detects which signal is stronger and pick it up), massive MIMO (using hundreds of ports for transmitting in base transceiver stations (BTSs)) combined with other previously mentioned techniques, full duplex and small cell networks (implementing many low power mini BTSs), etc. In addition, the millimeter-wavelength band in satellite communication would require a redesign and/or replacement of all communication instruments and devices, as well as a change to the present centimeter band satellite spectrum. This issue will rely critically on constructing an incentive auction that places a substantial premium on satellite sector share and asset value.

With certain conditions, the patterns of smart/phased array antennas can also be controlled more efficiently by optimization-based algorithm. Typically, these parameters are set to maximize the signal-to-interference ratio (SIR), minimize variance, reduce mean-square error (MSE), direct toward a signal obtained, or null depth to avoid signal interference. Also, they can be used to monitor moving emitters and interference in both static and dynamic geometries. Some of the canonical approaches in smart antennas are the least mean squares (LMS), sample matrix inversion (SMI), recursive least squares (RLS), conjugate gradient method (CGM), constant modulus algorithm (CMA), and the least squares constant modulus algorithm (LS-CMA). Instead of applying the time-consuming optimization process for beam shaping, look-up tables can also be used. It is also possible to build, design, and implement all these features on Radio Frequency Integrated Circuits (RFICs).

2. SMART ANTENNAS AND ANTENNA FEEDING NETWORKS

Smart antenna systems and beamforming applications (as the most important part of it) consist of military, industrial, health, etc. They are a crucial component of the next generation of mobile communication and radar systems. Smart antennas are currently being used in mobile communications to enhance the capacity of communication channels that are optimized in terms of performance and power, which has encouraged research and development in this interesting subject. Therefore, optimization, implementation, hybridization, and combination in these systems are critical.

Furthermore, because of smart antennas' diverse applications and the current demands to boost channel capacity in the fast-growing sector of mobile communications, research and development

activities in this subject around the world have sparked significant interest among researchers and engineers for decades. Smart antennas can identify and locate an undersea source of sound, such as a submarine, without needing active sonar because of this feature. Spatial filtering is a feature of smart antennas that allows them to take radiation from one direction while preventing it from another. Moreover, their capacity to direct transmitting energy in a precise direction makes them useful for medical diagnosis as well. This property also makes them extremely handy for neutralizing an unwanted jamming signal. A transmitter in a communication system generates an undesired jamming signal in the opposite direction of the intended signal. A typical application of array/optimum processing in smart antennas is to maximize the output signal-to-noise ratio (SNR). The beam pattern of the optimized array has the desired response in the signal direction while having a reduced response in the unwanted interference directions. Many different types of smart antenna processors have been proposed, and their performance has been investigated.

In this paper, a high-power UHF phase shifter for phased array antenna is designed. The design of a smart antenna array operating in the 600–1000 MHz frequency spectrum is explained in its physical layer, and the view of antenna array system analysis and design is also clarified in detail. The antenna system's pattern can scan from −60 to 60 degrees in elevation. Also, to cover the entire distance from the antenna, transmission power in BTSs (UHF transmitters) is typically 200 W (up to 1 MW). The processing unit (FPGA/Microcontroller) controls amplifiers, phase shifters, digital attenuators, etc. through an optimal algorithm to prevent interference and have the optimum coverage and intensify the signal power. As a result, the best weights, amplitudes, and phases are given to the antenna elements to achieve the best efficiency (Fig. 6).

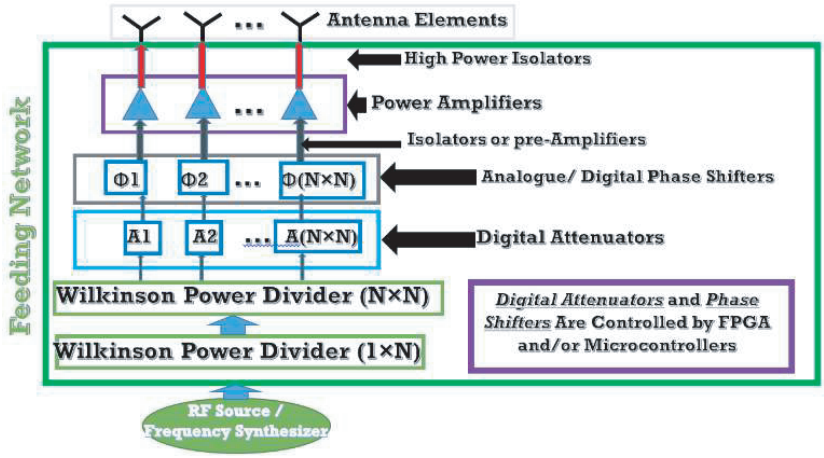

Figure 6. The block diagram of a typical high power smart antenna array.

2.1. Array Processing and Beamforming Techniques

As mentioned in previous sections, array processing in the receivers and beamforming techniques in transmitters and/or receivers can be used when we want maximum signal to noise ratio from data that are gathered from array antenna elements and cancelling interferences. It has many applications such as Radar (signal detection, direction of finding and speed detection, electronic war, etc.), radio astronomy, sonar, communication (mobile), direction finding systems (passive and active), medical diagnosis, and treatment and hospital instruments (for example for preventing unwanted receiving or signal interferences), etc. Array processing also has a critical role in array antenna systems, since analyzing input data and interferences or unwanted signals can help to find the required transmitter and/or receiver array antenna pattern and other RF specifications like transmitter power, receiver sensitivity, etc. A review on beamforming is mentioned/explained briefly in the following because illustrating all techniques, algorithms, and methods are beyond the scope of this paper.

Furthermore, antenna feeding networks and beamformings are designed for power and phase distributions of array antenna elements. In the feed lines of the array antenna elements, asymmetric

power dividers or analogue or digital attenuators can be utilized to design asymmetric power distributions. Also, phase distribution can be designed by phase shifters (analogue/digital/fiber optic phase sifters). Some of the most well-known fixed antenna feeding network methods are: *Rotman lens, McFarland 2D Matrix, Blass matrix, and Butler matrix.*

2.2. Traditional Amplitude Distribution

For amplitude distribution of array antenna elements, methods with predefined functions (have coefficients and specific known functions) can be used. These methods suppose symmetrical (or shifted symmetrical) amplitude distributions. Typical traditional methods are: Taylor, Dolph-Chebyshev, Binomial.

2.3. High Power Feeding Network Design

In communication systems, phase shifters are imperative parts. The specifications of a high performance phase shifter consist of: low insertion loss, high input and output return losses, a wide phase shifting range, and high phase resolution [11–20]. In all of these devices, changing the lengths of the transmission lines, continuously or by high power switches, create the requisite values of phase shifts or delay lines. Phase shifters are utilized for beamforming and 3D scanning in array antennas by controlling the relative phase of individual radiating elements. There are various types of them such as switched type and reflection-type ones. Base station antennas often include dual polarized/crossed dipole linear or planar arrays, and to change the down tilt angle of the array antenna beam, a phase shifter is applied [21–24]. In high power, a high power phase shifter has to be used.

High power phase shifters use high power PIN diodes to achieve high power capacity. For designing them, one way is using transmission (delay) line phase shifters. To put it another way, different lengths of transmission lines can be employed to achieve different phase shifts. Selecting each phase shift is prepared by high power microwave switches. The phase shifter is made up of only eight diodes arranged in microstrip circuit to keep prices down [25]. For high-power applications, a four-bit high-power UHF diode phase shifter can be used. These high power phase shifters can tolerate more than 4 kW pulse/1 kW CW (RF) signal (Fig. 7). Transmission lines are diverse, and they can be used in

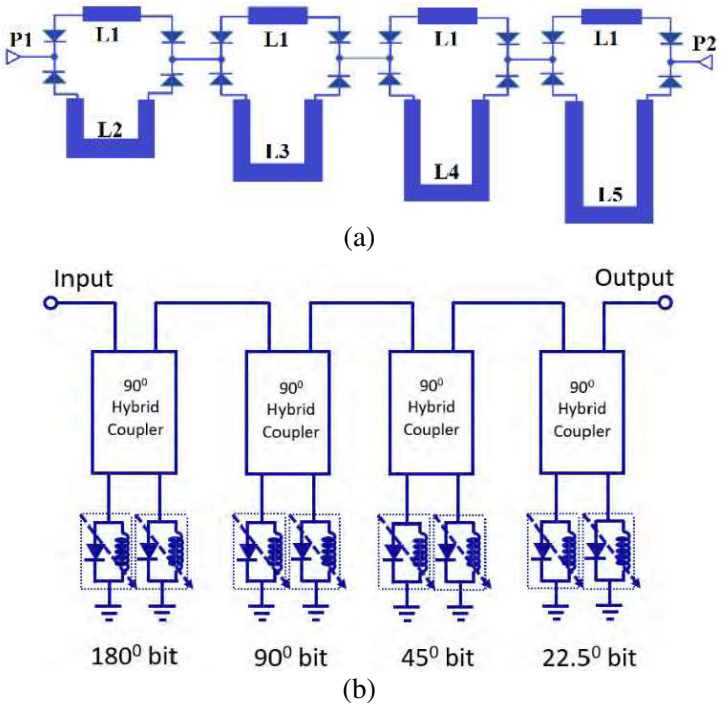

Figure 7. Four bit UHF diode phase shifter [25].

various forms such as microstrip/coaxial/stripline. As a result, by combining high-power delay lines with high-power microwave switches, the problem of power handling of the phase shifters can be solved. The insertion losses of these switches are less than 0.5 dB.

Furthermore, to achieve a standard 0.5-degree angle resolution phase shifter (with a typical antenna element spacing of 11 inches), minimum or the required accuracy phase shift and number of phase shifters for designing high power (diode/switch) phase shifters have to be computed (a typical wavelength = 37.5 cm in center frequency of 800 MHz). To do so, the array factor has to be considered [7]. The normalized array factor of a planar array is (a linear array only needs the progressive phase for one direction):

$$AF(\theta,\phi)_n = \left\{\frac{1}{M}\frac{\sin\frac{M}{2}\psi_x}{\sin\frac{\psi_x}{2}}\right\}\left\{\frac{1}{N}\frac{\sin\frac{N}{2}\psi_y}{\sin\frac{\psi_y}{2}}\right\} \tag{1}$$

where $\psi_x = kd_x\sin\theta\cos\phi + \beta_x$, $\psi_y = kd_y\sin\theta\sin\phi + \beta_y$.

If it is desired to have only one main beam that is directed along $\theta = \theta_0$ and $\phi = \phi_0$, the progressive phase shift between the elements in the x- and y-directions must be equal to:

$$\beta_x = -kd_y\sin\theta_0 cox\phi_0; \quad \beta_y = -kd_y\sin\theta_0\sin\phi_0 \tag{2}$$

The minimal required phase difference/progressive phase between antenna elements creates minimum phase shift. It occurs while switching from $\theta = 0$, $\phi = 0$ to $\theta = 0.5°$, $\phi = 0$. Phase change can be calculated from $\varphi_t = \beta_x + \beta_y$ (typically $d_x = d_y = 3\lambda/4$): $\beta_x + \beta_y = -180° \times \sin(0.5°) = 2.3° \sim -2$ degrees.

This is the angle resolution that is required. Required phase shifters for covering 360 degrees are: 2, 4, 8, 16, 32, 64, 128, 256 degrees. If RT/duroid 6010 substrate ($\varepsilon_r = 10.2$) is used in the designing process (for more compactness), maximum length for reaching the phase shift of 256 degrees is 10 cm. Also, as a typical example, the maximum required phase shift of a linear phased array (with $d = \lambda/2$) for beam tilt of 60 degrees is: $kd = -180$: $\beta(z) = -k \times d \times [\cos(\theta_0)] \sim -90$ degrees.

Three special features of 5G represent huge hurdles to test equipment and techniques compared to standard testing in the 3G/4G era:

- The use of millimeter-wave bands as well as microwave above 6 GHz.
- Ultra-wideband signal generating, receiving, and storing with bandwidths of hundreds of MHz or perhaps even GHz.
- Large-scale antenna arrays of 64, 128 or more channels: specification, design, and application.

Massive MIMO, a fundamental 5G technology, decreases transmission power while increasing channel capacity and spectral efficiency. Despite this, the number of network equipment antennas required is 10 to 100 times that of existing MIMO system antennas, creating a substantial bottleneck in the upgrade and optimization of current 4G/LTE/5G channel emulators. In the following parts, the goal is to design and simulate a smart array antenna system for a typical frequency of 800 MHz. The new UHF phased array TV-based 5G network not only prepares a solution for implementing ultra-wideband communication systems, but also exploits the existing hardware and software facilities to satisfy the booming needs. The high-power system can be designed and manufactured using high-power phase shifters and can be replaced by another high power switch type phase shifter represented in the next section.

3. HIGH POWER PHASE SHIFTER DESIGN

As explained, a high power phase shifter is needed to transfer the high power RF signal. To do so, in addition to the mentioned phase shifters in previous sections, electromechanical phase shifter is another solution which can also handle more RF power. Its structure includes a main Printed Circuit Board (PCB), moving one which rotates above the main PCB. The RF signal is capacitively coupled to the wiper PCB. To have less side lobe levels in the final antenna radiation pattern, an asymmetric power divider has to be used. When the upper PCB rotates, the path lengths of the RF signal also will vary and lead to changing of the output signals' phases.

A high power mechanical phase shifter is designed and investigated in this section. First, the structure of the high power phase shifter with asymmetric power dividing capability is illustrated. Next, the amount of power handling will be calculated and estimated.

3.1. Phase Shifter Design

In Figs. 8–9, the configuration of a typical rotational phase shifter is shown. Three arc-shaped strip lines make up this structure, constituted on a dielectric substrate. In other words, the variable phase shifter system with at least one primary PCB with an input trace coupled to a movable (rotational) junction is used in a panel antenna. The moveable PCB is linked to the primary PCB near the movable junction of this phase shifter. Of course, the gap between them is insignificant (air layer). A nonconductive coating covers the conductive arcs and movable conductive component is utilized to reduce inter-modulation distortion (IMD) and for insulating. Moreover, the thickness of the coating and dielectric must be adjusted to achieve the requisite capacitive coupling between the movable traces and corresponding main PCB traces.

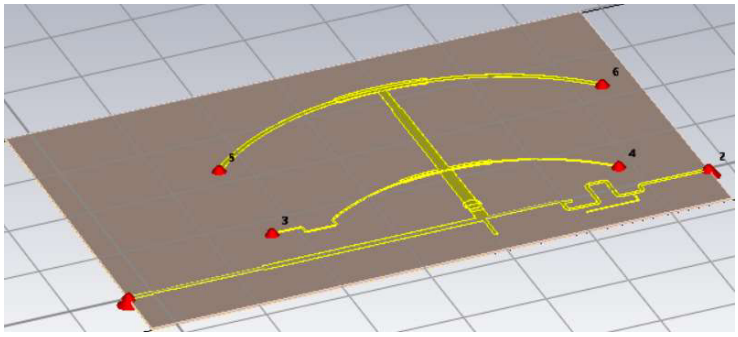

Figure 8. Configuration of the proposed rotational phase shifter.

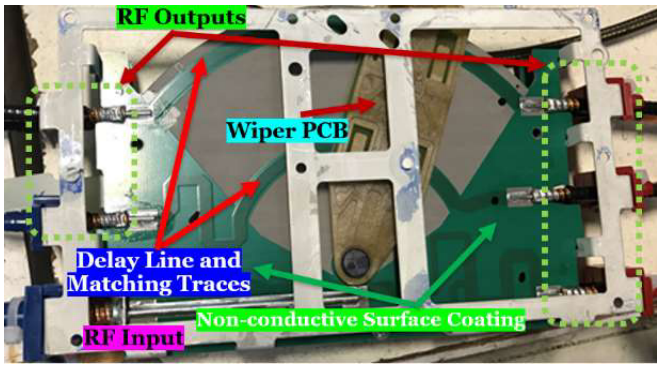

Figure 9. The proposed manufactured rotational phase shifter.

The phase shift is changed by the change in the outer arc's path length in the main PCB. It comprises multiple extra outputs with configurable phase shifts between them and fixed tapering amplitudes. The phases depend upon the position of the movable PCB. There is a conductive portion of movable PCB to transmit the input signal to the conductive arcs. The phase shifter receives signals through an input port and transmits them to a set of output ports. At the arc lines, the maximum line length is determined by the required beam tilting angle (maximum feed phase). Varied phase shifts result in different delay/transmission line lengths for ports connected to different arcs as follows:

$$-\frac{2\pi R_1(\theta)}{\lambda} \tag{3}$$

where $R_1(\theta)$ is the length of the outer arc from the center, and λ is the wavelength of the signals. The radius of the annular coupling region and the radius of the longest conductive arc can be computed using the following formula:

$$R = \frac{(N-1)d\sin(\beta_{\max})}{4\theta_{\max}\sqrt{\varepsilon_{eff}}} \tag{4}$$

where $\beta_{\max}$ is the maximum antenna beam steering angle, d the distance between adjacent antenna elements, $\theta_{\max}$ the maximum angle of rotation of the movable PCB, ε_{eff} the effective dielectric constant of the printed circuit board, and N the number of antenna elements. The coating material can be soldermask or another conformal coating, which can be placed while a PCB(s) are being silkscreened and UV cured. For the thin non-conductive layer, Humiseal coating polymers, available from Chase Corp's Humiseal Division in Pittsburgh, can be applied cheaply via dipping, spraying, or other liquid coating techniques. The conductive arc can also be created and configured as an airline, although this comes at the cost of the phase shifter height and antenna compactness. Also, the higher the dielectric constant the substrates have, the more compact the structure becomes. According to the required transmitted power, any low-cost substrate can be used in manufacturing process.

For amplitude tapering, the high-power phase shifter must have an asymmetric power distribution. Consider the three-port power divider depicted in Fig. 10, where k is the proportion of power in the first arm [26]. The number of impedance levels for the two transmission lines is the initial step in the design. A relation between Z_{02} and Z_{03} can be determined from:

$$k = \frac{Z_{03}}{Z_{02}+Z_{03}}; \quad \frac{Z_{i2}Z_{i3}}{Z_{i2}+Z_{i3}} = Z_0 \tag{5}$$

For a three-port power divider perfectly matched at port 1, holds and expressions linking the equivalent impedances Z_{i2} and Z_{i3} are written as:

$$(Z_{02})^2 = Z_0 Z_{i2}; \quad (Z_{03})^2 = Z_0 Z_{i3} \tag{6}$$

The final design equations are as follows:

$$Z_{03} = Z_0\sqrt{\left[1+\left(\frac{k}{1-k}\right)^2\right]}; \quad Z_{02} = \frac{1-k}{k}Z_{03}; \quad R_p = 2Z_0 \tag{7}$$

In the above design equations, if the power-split ratio is 2, $k = 1/3$.

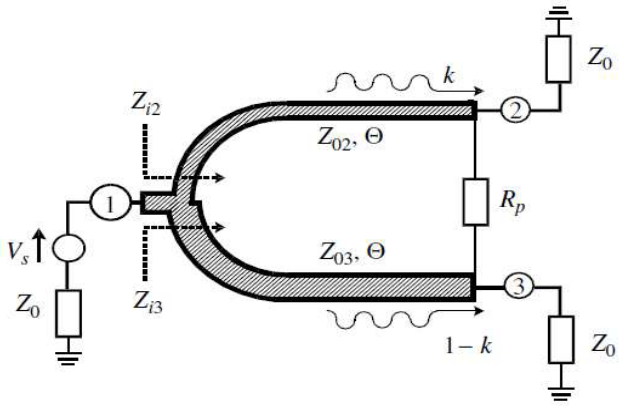

Figure 10. Power divider with configurable power divisions.

3.2. Power Handling

The multipactor parameter (a high power RF breakdown occurring in vacuum or near vacuum microwave systems) is a criterion in high power systems and has been analyzed and obtained in some structures including reflect arrays, transmission lines, etc. [27–30]. In the multipactor discharge, electrons are

accelerated by the electromagnetic fields. Increasing them leads to exponential charge growth and ultimately electron discharge. In other words, multipactor is caused by multiple secondary electron emissions due to repeated (multiple) electron impact onto material surfaces. Its effects range from signal degradation to the complete destruction of the component.

On the other hand, the average power handling capability (APHC) of a microstrip, like that of any other dielectric filled transmission line, is limited by the heating caused because of ohmic and dielectric losses [31–34]. In fact, the APHC of a multilayer microstrip is affected by parameters comprising: (a) the transmission line losses, (b) the thermal conductivity of the dielectric layers and the substrate material, (c) the surface area of the strip conductor, (d) the maximum allowed operating temperature of the microstrip structure, and (e) the ambient temperature, that is, the temperature of the medium surrounding the microstrip. Briefly, the power handling of a (multilayer) microstrip structure is computed as follows:

$$P_{avg} = (T_{\max} - T_{amb})/\Delta T \tag{8}$$

where ΔT is the maximum working temperature, and $T_{\max}$ signifies the temperature increase per watt. Additionally, microstrip circuits' maximum operational temperature is limited by (a) substrate qualities with temperature, (b) physical dimensions with temperature, and (c) connectors. We also have:

$$\Delta T = T - T_{amb} = 0.2303\left[\alpha_c\left(\frac{h}{W_e K_d} + \frac{d}{W_e K_a}\right) + \alpha_d\left(\frac{h(h+2d)}{2W_e K_d(h+d)} + \frac{d^2}{W_e K_a(h+d)}\right)\right] \tag{9}$$

where K_d and K_a are the thermal conductivities of the dielectric substrate and the air layer, respectively. Also, T_{amb} is the ambient temperature, and α_d (dB/m) is the dielectric loss attenuation coefficient. (≈ 0.2), α_c (dB/m) is the attenuation coefficient due to loss in the strip conductor (which is small especially in VHF/UHF frequency band); h is the dielectric height; d is the air height; $W_e = 120\pi(h+d)/Z_0^a$; and Z_0^a is the microstrip impedance with air as the dielectric. According to formula (3), for $T_{\max} = 150°\,\mathrm{C}$ $K_d = 0.7$ (thermal conductivity of RO4003), $h = 0.5\,\mathrm{mm}$ and $Z_0 = 50$, the average power handling is more than 20 kW in the UHF/VHF frequency band (when it is packed in vacuum). The maximum power handling of the structure can be increased to more than 1 MW by using a thinner substrate, thicker strip conductor, using vacuum box, and modifying the physical dimensions of the transmission lines. This can be employed in TV-based 5G systems in remote areas. Also, according to the RO4003 specifications, the electrical strength of the substrate is 31.2 kV/mm.

According to vacuum breakdown simulations with CST STUIO SUITE SPARK3D (Fig. 11), it is expected that a microstrip line on the RO4003 substrate is able to handle more than 50 kW of RF power. Fig. 12 illustrates the SPARK3D multipactor simulation results of the structure as well. There is no gap in the structure/microstrip/feed lines to affect the breakdown power. The figures depict the dependency of power handling to the working frequency. The reason is that the dielectric loss attenuation coefficient

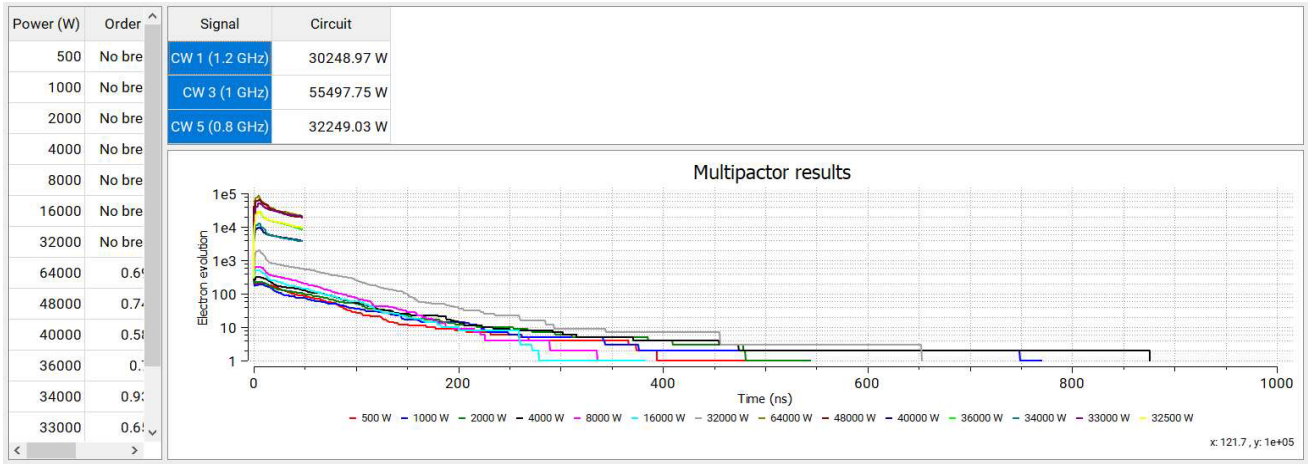

Figure 11. The multipactor results simulated by SPARK3D 2021 of a microstrip line.

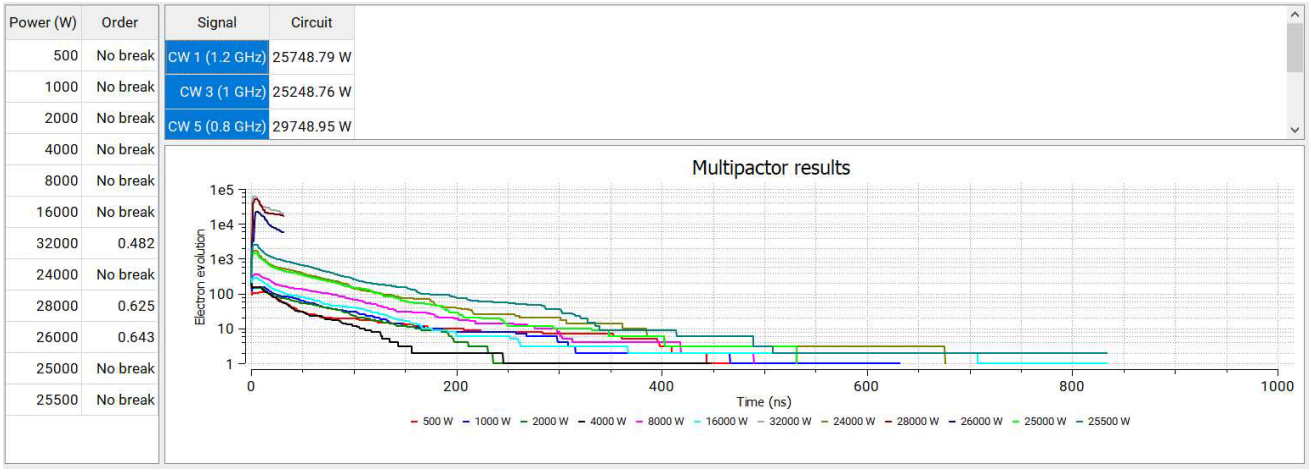

Figure 12. The multipactor results simulated by SPARK3D 2021 of the structure.

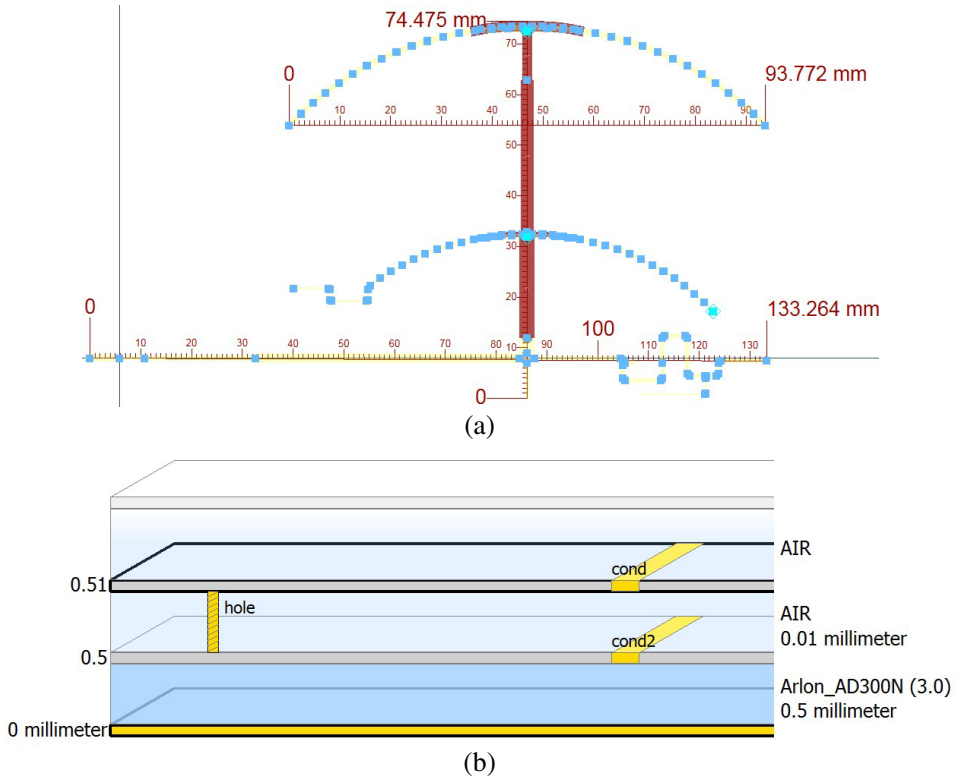

Figure 13. Layout and substrate specifications of the designed phase shifter.

is also frequency dependent. The breakdown in the structure depends on the physical dimensions of the structure too.

4. SIMULATION AND MEASURED RESULTS

Having analyzed the design methods and the calculations of the parameters explained above, the considered high power rotational phase shifter has been designed and fabricated. The ADS layout, simulation and measured results are depicted in Figs. 13–17. In the main transmission lines, the

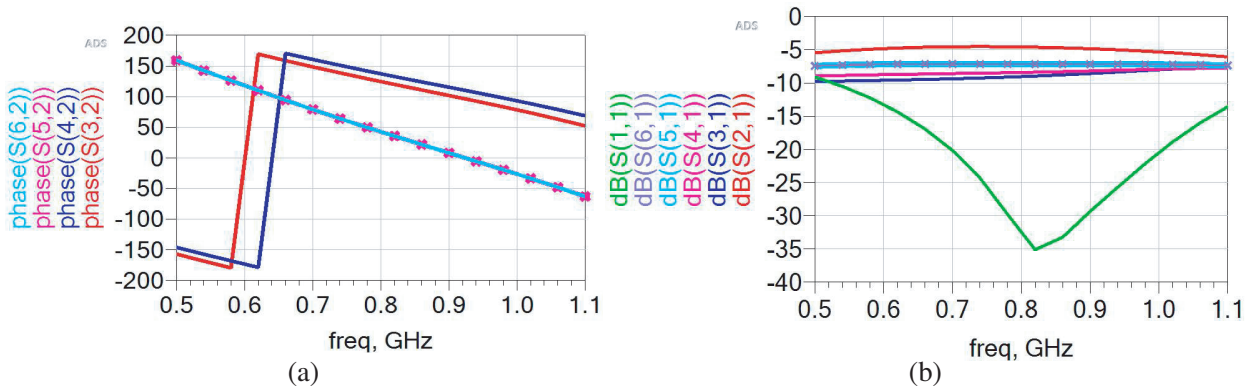

Figure 14. Simulation results of the rotational phase shifter in ADS in center position.

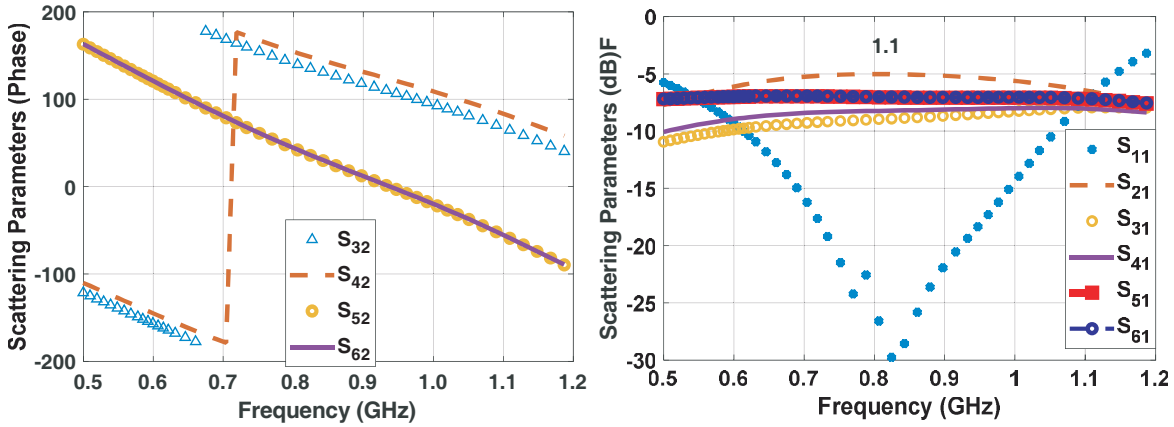

Figure 15. The rotational phase shifter's measurements in the center position.

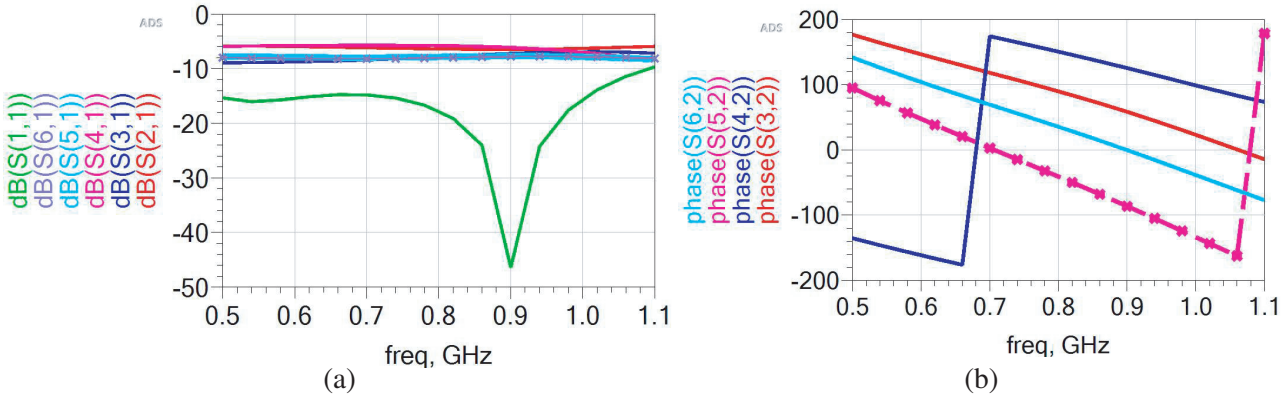

Figure 16. Simulation results of the rotational phase shifter in ADS in 45 degrees position.

characteristic impedance of the microstrip lines is 50, and in other transmission lines, it is determined by the power ratio required for amplitude tapering.

Because ADS software uses a momentum method solver that is optimized for microstrip and patch structures and runs electromagnetic simulations faster and better, simulations have been done by ADS. By using circuit models and design mathematical formulas, software like Microwave office (AWR), ADS,

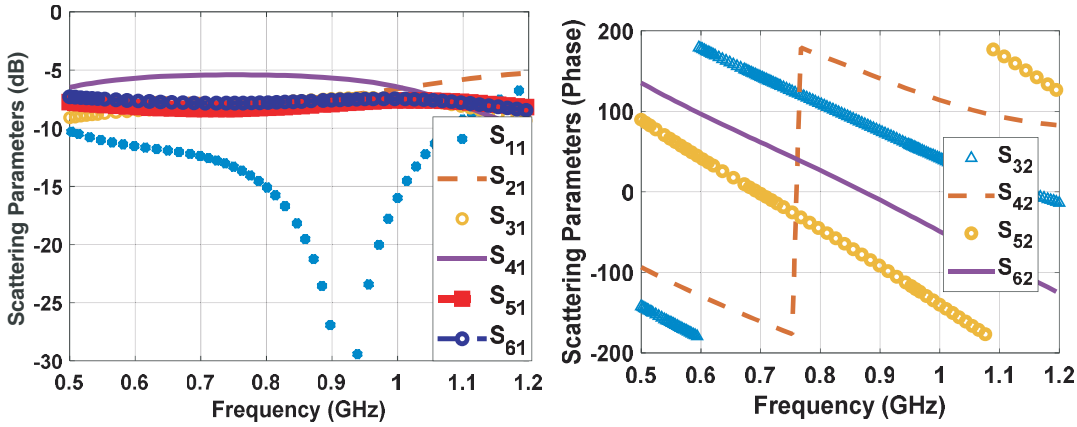

(a) (b)

Figure 17. Measured results of the rotational phase shifter in 45 degrees position.

CST can simulate and optimize microstrip and patch structures. HFSS and CST software are optimized for waveguide or huge structures and use FIT (Finite Integration Technique) and FEM (Finite Element Method) solvers respectively that are more time consuming. Last but not least, the phase shifter needs a mechanical motor for phase adjusting.

5. CONCLUSION

4G/5G/6G communication systems as the current have been optimized for upcoming generations of mobile data connectivity. The modern systems have been developing and progressing and will provide unbelievably fast broadband speeds such as TV-based 5G systems. But in some frequencies they also need high-power products. In sub-6 GHz cellular networks, a high-power phase shifter is designed, simulated, and manufactured. It has useful specifications like high power handling and beam tilting. By the similar design procedure, the antenna system can cover −60–60 degrees beam rotation of linear array antennas with any number of output ports. The structures designed for high power and linear or planar phased (smart) array antenna systems can be improved and redesigned similarly for other systems/structures/number of antenna elements and frequencies. By implementing smart systems and beam tilting, wireless interference cancellation is achieved which is very versatile and is utilized in identification systems, motion detection radars, and vehicle radars.

REFERENCES

1. Wang, J., J. Weitzen, O. Bayat, V. Sevindik, and M. Li, "Interference coordination for millimeter wave communications in 5G networks for performance optimization," *EURASIP Journal on Wireless Communications and Networking*, Vol. 2019, No. 1, 46, 2019.
2. Zhang, J., E. Björnson, M. Matthaiou, D. W. K. Ng, H. Yang, and D. J. Love, "Guest editorial special issue on multiple antenna technologies for beyond 5G — Part II," *IEEE Journal on Selected Areas in Communications*, Vol. 38, No. 9, 1941–1944, 2020.
3. Oskouei, H. R. D., A. R. Dastkhosh, A. Mirtaheri, and M. Naseh, "A small cost-effective super ultra-wideband microstrip antenna with variable band-notch filtering and improved radiation pattern with 5G/IoT applications," *Progress In Electromagnetics Research M*, Vol. 83, 191–202, 2019.
4. Azimzadeh, M. and G. Jelodar, "Trace elements homeostasis in brain exposed to 900 MHz RFW emitted from a BTS-antenna model and the protective role of vitamin E," *Journal of Animal Physiology and Animal Nutrition*, Vol. 104, No. 5, 1568–1574, 2020.
5. Letaief, K. B., W. Chen, Y. Shi, J. Zhang, and Y.-J. A. Zhang, "The roadmap to 6G: AI empowered wireless networks," *IEEE Communications Magazine*, Vol. 57, No. 8, 84–90, 2019.

6. Varrall, G., *5G Spectrum and Standards*, Artech House, 2016.
7. Balanis, C. A., *Antenna Theory: Analysis and Design*, John wiley & sons, 2016.
8. Hansen, R. C., *Phased Array Antennas*, Vol. 213, John Wiley & Sons, 2009.
9. Sim, M. S., Y.-G. Lim, S. H. Park, L. Dai, and C.-B. Chae, "Deep learning-based mmWave beam selection for 5G NR/6G with sub-6 GHz channel information: Algorithms and prototype validation," *IEEE Access*, Vol. 8, 51634–51646, 2020.
10. Jaeschke, T., C. Bredendiek, S. Küppers, and N. Pohl, "High-precision D-band FMCW-radar sensor based on a wideband SiGe-transceiver MMIC," *IEEE Transactions on Microwave Theory and Techniques*, Vol. 62, No. 12, 3582–3597, 2014.
11. Li, W.-T., Y.-C. Chiang, J.-H. Tsai, H.-Y. Yang, J.-H. Cheng, and T.-W. Huang, "60-GHz 5-bit phase shifter with integrated VGA phase-error compensation," *IEEE Transactions on Microwave Theory and Techniques*, Vol. 61, No. 3, 1224–1235, 2013.
12. Zheng, Q., Z. Wang, K. Wang, G. Wang, H. Xu, L. Wang, W. Chen, M. Zhou, Z. Huang, and F. Yu, "Design and performance of a wideband Ka-band 5-b MMIC phase shifter," *IEEE Microwave and Wireless Components Letters*, Vol. 27, No. 5, 482–484, 2017.
13. Dey, S., , S. K. Koul, A. K. Poddar, and U. L. Rohde, "Reliable and compact 3-and 4-bit phase shifters using MEMS SP4T and SP8T switches," *Journal of Microelectromechanical Systems*, Vol. 27, No. 1, 113–124, 2018.
14. Garg, R. and A. S. Natarajan, "A 28-GHz low-power phased-array receiver front-end with 360° RTPS phase shift range," *IEEE Transactions on Microwave Theory and Techniques*, Vol. 65, No. 11, 4703–4714, 2017.
15. Gu, P. and D. Zhao, "Ka-band CMOS 360° reflective-type phase shifter with±0.2 dB insertion loss variation using triple-resonating load and dual-voltage control techniques," *2018 IEEE Radio Frequency Integrated Circuits Symposium, RFIC)*, IEEE, 2018.
16. Kalyoncu, I., E. Ozeren, A. Burak, O. Ceylan, and Y. Gurbuz, "A phase-calibration method for vector-sum phase shifters using a self-generated LUT," *IEEE Transactions on Circuits and Systems I: Regular Papers*, Vol. 66, No. 4, 1632–1642, 2019.
17. Guomin, D. I. N. G., M. Zimmerman, J. Yu, and H. Qin, "Base station antennas including wiper phase shifters," U.S. Patent No. 11,081,789, Aug. 3, 2021.
18. Timofeev, I. E., M. L. Zimmerman, and X. Ai, "Phase shifter and antenna including phase shifter," U.S. Patent No. 7,907,096, Mar. 15, 2011.
19. Schmutzler, S., "Cellular antenna phase shifter positioning using motorized torque lever," U.S. Patent Application No. 12/771,826.
20. Ko, Y.-H., "Distributed antenna system interface tray," U.S. Patent No. 10,123,282, Nov. 6, 2018.
21. Farasat, M., D. N. Thalakotuna, Z. Hu, and Y. Yang, "A review on 5G sub-6 GHz base station antenna design challenges," *Electronics*, Vol. 10, No. 16, 2000, 2021.
22. Wu, Z., B. Wu, Z. Su, and X. Zhang, "Development challenges for 5G base station antennas," *2018 International Workshop on Antenna Technology (iWAT)*, IEEE, 2018.
23. Yang, Y. and Z. Hu, "Advanced multifunctional antennas for 5G and beyond," *2019 Photonics & Electromagnetics Research Symposium — Fall, PIERS — Fall)*, 2019.
24. Zhang, X., F. Sun, G. Zhang, and L. Hou, "Compact UHF/VHF monopole antennas for CubeSats applications," *IEEE Access*, Vol. 8, 133360–133366, 2020.
25. Trinh, K. T., J. Feng, S. H. Shehab, and N. C. Karmakar, "1.4 GHz low-cost PIN diode phase shifter for L-band radiometer antenna," *IEEE Access*, Vol. 7, 95274–95284, 2019.
26. Ahn, H.-R., *Asymmetric Passive Components in Microwave Integrated Circuits*, Vol. 182, John Wiley & Sons, 2006.
27. Roper, J. S. and A. F. Peterson, "Reflectarray power handling capability analysis," *2022 IEEE International Symposium on Antennas and Propagation and USNC-URSI Radio Science Meeting, AP-S/URSI)*, IEEE, 2022.
28. Vaughan, J. and M. Rodney, "Multipactor," *IEEE Transactions on Electron Devices*, Vol. 35, No. 7, 1172–1180, 1988.

29. Kim, H. C., J. P. Verboncoeur, and Y. Y. Lau, "Invited paper — Modeling RF window breakdown: From vacuum multipactor to RF plasma," *IEEE Transactions on Dielectrics and Electrical Insulation*, Vol. 14, No. 4, 774–782, Aug. 2007.
30. Anza, S., M. Mattes, C. Vicente, J. Gil, D. Raboso, V. E. Boria, and B. Gimeno, "Multipactor theory for multicarrier signals," *Physics of Plasmas*, Vol. 18, No. 3, 032105, 2011.
31. Bahl, I. J., "Average power handling capability of multilayer microstrip lines," *International Journal of RF and Microwave Computer-Aided Engineering: Co-sponsored by the Center for Advanced Manufacturing and Packaging of Microwave, Optical, and Digital Electronics, CAMPmode) at the University of Colorado at Boulder*, Vol. 11, No. 6, 385–395, 2001.
32. Bahl, I. J. and K. C. Gupta, "Average power-handling capability of microstrip lines," *IEE Journal on Microwaves, Optics and Acoustics*, Vol. 3, No. 1, 1–4, 1979.
33. Garg, R., I. Bahl, and M. Bozzi, *Microstrip Lines and Slotlines*, Artech House, 2013.
34. Parnes, M., "The correlation between thermal resistance and characteristic impedance of microwave transmission lines," *Microwave Journal*, Vol. 43, No. 3, 82–82, 2000.